frontiers | Frontiers in Environmental Science

TYPE Original Research
PUBLISHED 17 January 2025
DOI 10.3389/fenvs.2024.1502552

OPEN ACCESS

EDITED BY
Christophe Darnault,
Clemson University, United States

REVIEWED BY
Mahsa Ghorbani,
Clemson University, United States
Fuping Li,
North China University of Science and Technology, China
Yiqie Dong,
Wuhan Polytechnic University, China

*CORRESPONDENCE
Fenglan Han,
2002074@nmu.edu.cn

RECEIVED 27 September 2024
ACCEPTED 27 December 2024
PUBLISHED 17 January 2025

CITATION
Liu Y, Han F, Li N, Dong F, An C, Yang W and Li T (2025) Study on the synergistic preparation of functional soil from multiple coal-based solid wastes.
Front. Environ. Sci. 12:1502552.
doi: 10.3389/fenvs.2024.1502552

Study on the synergistic preparation of functional soil from multiple coal-based solid wastes

Yanan Liu[1], Fenglan Han[1,2]*, Ning Li[1], Fuyuan Dong[1], Changcong An[3], Wenna Yang[4] and Tingfeng Li[4]

[1]Institute of Materials Science and Engineering, North Minzu University, Yinchuan, China, [2]International Scientific and Technological Cooperation Base of Industrial Waste Recycling and Advanced Materials, Yinchuan, China, [3]Institute of New Materials Technology, University of Science and Technology Beijing, Beijing, China, [4]Land Management Project Section, Ningxia Agricultural Comprehensive Development Centre, Yinchuan, China

Three coal-based solid wastes—fly ash (FA), gasification slag (GS), and coal gangue (CG)—were used to prepare functional soil (FGC) for the ecological restoration of mining areas. It not only solves the problem of shortage of soil resources in the mining area, but also realizes the resourceful use of coal-based solid waste. Investigating the functional soil physicochemical properties and oatgrass growth characteristics revealed the optimal functional soil ratios. Compared with the control (CK) at 30 d, the average pH of the FGC3 (FA: 50wt%; GS: 25wt%; CG: 25wt%) decreased from 9.54 to 8.54, the average organic matter content increased from 2.57% to 7.60%, and the average available potassium and ammonium nitrogen content increased from 38.02 to 2.83 mg·kg^{-1} to 53.46 and 3.21 mg·kg^{-1}, respectively. Functional soil bulk density and porosity were superior to Sandy soil somewhere in Ningxia (SL) for GS and CG contents <25wt%. GS and CG significantly improved oatgrass agronomic traits. Compared with CK the average plant height, stem thickness, fresh weight, and dry weight of oatgrass in FGC3 increased from 17.68 cm, 0.99 mm, 0.09 g, and 0.02 g to 27.0 cm, 1.26 mm, 0.24 g, and 0.04 g, respectively. And chlorophyll content was increased by 20.39% compared with CK. This study verified the feasibility of the synergistic preparation of functional soils from three coal-based solid wastes and provides reference for the ecological restoration and large-scale utilization of coal-based solid wastes.

KEYWORDS

coal-based solid waste, functional soil, physical properties, chemical properties, agronomic traits

1 Introduction

The majority of China's open-pit coal mines are concentrated in the arid and semiarid regions in the north (Yuan et al., 2022). The development and utilization of mineral resources have caused serious ecological degradation and environmental pollution, restricting the economic development of arid regions while promoting economic development (Chen et al., 2022). After continuous large-scale mining and abandonment, the mines have seriously damaged the ecosystems, with impacts including an increase in soil heavy-metal content, a decrease in vegetation cover, dust

pollution, and soil erosion (Vinayagam et al., 2024). Despite the recent achievements in the recovery of mining areas in arid areas, in the long run, the ecological restoration capacity of mining areas is still relatively weak, mainly manifested in low vegetation cover-age and survival rates, and insignificant ecological environment improvement (Xu et al., 2023). Vegetation restoration in mining areas can effectively improve the physical and chemical properties of soil, restore the landscape of mining areas, and promote the sustainable development of the economy and ecology.

Coal-based solid waste is a by-product of coal mining, processing, combustion, and conversion processes, and mainly includes fly ash (FA), coal gangue (CG), desulphurization gypsum, and gasification slag (GS) (Zhang J. et al., 2022). The annual emissions of FA in China have exceeded 780 million tons (Chao et al., 2023), the annual output of GS is more than 60 million tons (Zhu et al., 2020). By 2020, the cumulative amount of CG in the country has exceeded 6 billion tons (Shuai et al., 2022). The massive accumulation of coal-based solid waste causes continuous pollution and damage to the surrounding environment, water, and soil (Wang and Cheng, 2024). At present, FA, GS, and CG are mainly used in construction building materials, roadbed construction, etc. (Zhang et al., 2024). However, with the development of the industrial economy, the output of these wastes is much larger than the demand for their utilization. Thus, there is an urgent need to develop new uses for coal-based solid waste. The main components of FA are Al_2O_3 and SiO_2, which are similar to natural clays and contain trace elements necessary for plant growth (e.g., B, Fe, Mo, Cu, Mn, and Zn) (Ou et al., 2020; Panda et al., 2021). CG contains large amounts of carbonaceous shale and siltstone, which are rich in nutrients such as nitrogen, phosphorus, potassium, silica, and organic matter essential for plant growth (Luo et al., 2024). GS is rich in calcium, magnesium, and silicon, as well as amorphous aluminosilicates, which are soluble in soil and can be absorbed and utilized by plants (Zhang et al., 2023). The application of coal-based solid waste in agriculture has received much attention in recent years. For example, Rusanescu and Rusanescu (2023) planted onions on soil with different concentrations of added FA. The authors showed that the soil pH increased from 7 to 8.2 and the electrical conductivity, organic carbon and organic matter, and soil water-holding capacity of the soil were enhanced following the application of the ash. Liu et al. (2022) addition of gasified slag to acidic soils, and found that the particle size composition of the acidic soil significantly improved, the soil bulk weight decreased by 3.38%–28.12%, and the water retention and water-holding capacity of acidic soil significantly were enhanced. Du et al. (2020) used gangue, soil, corn stover, FA, and water retention agents to prepare a new type of planting substrate in orthogonal experiments. The results showed that the addition of gangue significantly improved the chemical indexes of the substrate, and alfalfa growth was promoted with the addition of 500 g.

Overall, FA, GS, and CG have elements required for plant growth and can be used as effective soil conditioners, and theoretically can also be used to prepare functional soils for ecological restoration in mining areas. However, previous studies have mainly applied coal-based solid wastes such as fly ash and gasifier slag as additives to the soil, with the aim of improving the soil, and have not adequately solved the problem of soil shortage in mining areas. At present, the amount of fly ash, gasification slag and coal gangue used for soil improvement is relatively small, and there are few studies on the collaborative preparation of multiple solid wastes for ecological rehabilitation of mining areas. Therefore, it is of great significance to explore and develop new ways to utilize coal-based solid wastes, and the direct preparation of functional soil from coal-based solid wastes for ecological restoration in mining areas not only improves the large-scale utilization of bulk industrial solid wastes, but also effectively solves the problem of shortage of planting soils in mining areas, and provides guidance to ecological environment restoration in mining areas. Therefore, in this study three kinds of coal-based solid wastes (FA, GS, CG) were used to prepare functional soil (FGC) after removing heavy metals. The changes of physical and chemical properties of different functional soils and agronomic characters of oat grass were discussed, and compared with sandy loam soil (SL) in Ningxia to screen out the more suitable ratio of functional soil for plant growth. The objectives of this study are (1) to evaluate the effects of different ratio of solid waste and action time on the physical and chemical properties of functional soils, (2) to evaluate the effects of different ratio of solid waste on the maximum water holding capacity and water loss rate of functional soils, and (3) to evaluate the effects of different ratios of functional soils on oatgrass plant height, stem thickness, fresh weight, dry weight, and chlorophyll content.

2 Materials and methods

2.1 Experimental material

FA, GS, and CG were obtained from a power plant in Ningxia after heavy metal removal. Tables 1–3 report the main components, basic physical and chemical properties, and heavy metal contents of the experimental raw materials, respectively. The tested heavy metal content is in accordance with the Chinese national standard "Soil environmental quality soil pollution risk control standards for agricultural land (for trial implementation)" (GB15618-2018) and can be employed for ecological restoration. The functional soil in this experiment is a sandy loam (SL) from a place in Ningxia as the reference value for the prepared functional soil. Table 4 reports the basic physicochemical properties of SL.

2.2 Experimental design

The experiment was conducted in April 2024 at room temperature conditions (temperature: 23°C, humidity 42%RH) in the laboratory of the School of Materials Science and Engineering, North Minzu University. As shown in Table 5, A total of 1 kg of fly ash was used as the control (CK), and FA, GS, and CG were mixed in different proportions to form 1 kg of functional soil (CK, FGC1, FGC2, FGC3, FGC4, and FGC5, respectively). After mixing, the soil was poured into plastic pots with an upper caliber of 16 cm, a bottom diameter of 12 cm, and a height of 11.5 cm. Each group was replicated nine times with a total of 54 pots. The experimental cycle was implemented under three time periods (10 d, 20 d, and 30 d). The functional soil was watered every 2 days to maintain a water content of 30% in each pot, and the irrigation water had a pH of 7.69 and an electrical conductivity (EC) of 669 $\mu S \cdot cm^{-1}$. The

TABLE 1 The main components of functional soil raw materials (wt%).

Properties	SiO_2	Al_2O_3	Fe_2O_3	CaO	MgO	K_2O	Na_2O
Content (FA)	45.91	21.80	4.27	3.24	1.24	2.17	0.84
Content (GS)	28.19	10.67	6.23	4.86	0.97	1.10	0.75
Content (CG)	50.76	19.61	4.74	3.71	1.61	2.04	1.18

TABLE 2 Basic chemical properties of functional soil raw materials.

Properties	pH	EC /(μS·cm^{-1})	Organic matter /%	Available phosphorus /(mg·kg^{-1})	Available potassium /(mg·kg^{-1})	Ammonium nitrogen /(mg·kg^{-1})
Content (FA)	10.97	1942	2.75	167.74	193.78	41.72
Content (GS)	7.70	360	2.16	29.71	80.89	2.73
Content (CG)	7.97	1416	21.16	6.21	308.39	3.01

TABLE 3 Comparison of the heavy metal content of functional soil raw materials and the risk control standard for soil pollution in agricultural land.

Properties	Hg /(mg·kg^{-1})	As/(mg·kg^{-1})	Pb /(mg·kg^{-1})	Cr /(mg·kg^{-1})	Cd /(mg·kg^{-1})	Ni /(mg·kg^{-1})
Content (FA)	0.343	16	98.4	102	0.59	41.7
Content (GS)	0.040	6.4	13.2	104	0.1	55.7
Content (CG)	0.0945	6.95	41.25	57.55	0.265	22.35
GB15618-2018	3.4	25	170	250	0.6	190

TABLE 4 Basic physical and chemical properties of SL.

Properties	pH	EC /(μS·cm^{-1})	Organic matter /%	Available phosphorus /(mg·kg^{-1})	Available potassium /(mg·kg^{-1})	Ammonium nitrogen /(mg·kg^{-1})	Bulk density /(g·cm^{-3})	Soil porosity /%
Content	8.46	176.7	6.19	23.31	123.98	2.44	1.31	41.99

physical indexes of the functional soil were measured with a 100 cm^{-3} ring knife at different incubation times. For the chemical soil properties, 200 g of the functional soil was sampled from each pot, air-dried naturally, and sieved through a 2 mm pore size. The chemical properties were determined after sieving.

2.3 Pot experiment

Oatgrass planting experiments were conducted in April 2024 at room temperature conditions (temperature: 23°C, humidity 42% RH) in the laboratory of the School of Materials Science and Engineering, North Minzu University. A total of 1 kg of fly ash was used as the CK, and FA, GS, and CG were configured into 1 kg of functional soil in different proportions (Table 5). Water was added to each pot to maintain the water content of the functional soil at 30% and the pots were left to stand for 2 d. Thirty oatgrass seeds were sown in the functional soil at a depth of 1–2 cm, and water was replenished every 2 days during the experimental cycle, with three replications of each proportion for a total of 18 pots. The experimental cycle was set at 30 d. Oatgrass-related agronomic traits were measured at 30 d of planting.

2.4 Test indicators and methods

2.4.1 Determination of the functional soil chemical properties

The pH value of the functional soil was determined by the potentiometric method (water: soil = 2.5:1), the EC was determined by the electrode method (water: soil = 5:1), the organic matter was determined by the loss on ignition method, and the available phosphorus and available potassium contents of functional soil were determined by ultraviolet-visible spectrophotometer (Carry6000i). The ammonium nitrogen content of functional soil was determined by the extraction–distillation method and the main raw material components were analyzed by an X-ray fluorescence spectrometer (AxiosPW4400).

TABLE 5 Raw materials and proportions of the functional soils.

Group number	FA/wt%	GS/wt%	CG/wt%
CK	100	0	0
FGC1	90	5	5
FGC2	70	15	15
FGC3	50	25	25
FGC4	30	35	35
FGC5	10	45	45

2.4.2 Determination of the maximum water-holding capacity and water loss rate of functional soil

The maximum water-holding capacity and water loss rate of the functional soil were measured at room temperature. The experiment was repeated three times. A total of 200 g of mixed functional soil (Table 5) was prepared in different proportions and poured into a PVC pipe with an inner diameter of 4.5 cm and a height of 15.5 cm. The bottom of the pipe was sealed with two layers of 200 mesh nylon cloth, and the weight was recorded as W1. Following this, 110 g of water was slowly added to the tube to slowly soak the functional soil until water seeped out from the bottom. When there was no water seeping out from the bottom of the tube, the tube mouth was sealed with plastic wrap, and the weight was recorded as W2. The tube was then weighed every day as Wi (i is the number of days of weighing) for 30 days. The formulas for calculating the maximum water holding capacity (MWH) and water loss rate (LR) of functional soil are shown in Equations 1, 2:

$$\mathrm{MWH}(\%) = ((\mathrm{W2} - \mathrm{W1}) \times 100)/200 \quad (1)$$

$$\mathrm{LR}(\%) = \left((\mathrm{W2} - \mathrm{Wi})/(\mathrm{W2} - \mathrm{W1})\right) \times 100 \quad (2)$$

where W2 is the weight of the PVC pipe bottom with no water seepage; W1 is the initial mass of the PVC pipe filled with mixed functional soil; and Wi is the daily weight (i is the number of days weighed).

2.4.3 Determination of the functional soil bulk density, porosity, and solid-liquid-gas ratio

A knife ring was placed vertically at the center of the soil in the flowerpot and pushed to slowly enter the soil. When it was completely filled with soil, the excess soil on the upper and lower edges was removed. The knife ring was covered with bottom and top covers and weighed (W1). It was then placed in a flat-bottomed container. Water was added to the container up to the upper edge of the knife ring and it was soaked for 10 h. It was then taken out, quickly wiped, and weighed (W2). The knife ring was placed on a stand for 12 h to allow gravity to drain the water and it was then weighed again (W3). After weighing, the knife ring was placed in a 105°C forced air drying oven, dried to constant weight, and weighed (W4). Equations 3, 5:

$$\text{Soil bulk density}\left(\mathrm{g \cdot cm^{-3}}\right) = (\mathrm{W4} - \mathrm{W0})/\mathrm{V} \quad (3)$$

$$\text{Soil porosity}(\%) = \left((\mathrm{W2} - \mathrm{W4})/\mathrm{V}\right) \times 100 \quad (4)$$

$$\text{Soil water content}(\%) = \left((\mathrm{W1} - \mathrm{W4})/(\mathrm{W1} - \mathrm{W0})\right) \times 100 \quad (5)$$

The ratio of solid, liquid and gas of functional soil is calculated based on the porosity and water content of functional soil, as shown in Equations 6–8:

$$\text{Solid phase}(\%) = 1 - \text{soil porosity} \quad (6)$$

$$\text{Liquid phase}(\%) = \text{soil porosity} - \text{soil water content} \quad (7)$$

$$\text{Gas phase}(\%) = 1 - \text{solid phase} - \text{liquid phase} \quad (8)$$

2.4.4 Determination of plant agronomic traits

The height of oatgrass was measured with a tape measure, the chlorophyll content was measured with a chlorophyll meter (TYS-B), the stem diameter was measured with a digital vernier caliper, and the fresh weight and dry weight were weighed with an analytical balance. The height and chlorophyll content of oatgrass were measured 30 d after planting, and then 10 above-ground components of each pot were randomly selected, rinsed with pure water, and weighed after being placed at room temperature for 2 h. The average value was recorded as the fresh weight of the oatgrass. The weight was determined after drying at 75°C for 24 h to a constant weight, and the average value was recorded as the dry weight of oatgrass.

2.5 Data analysis

Microsoft Office 2021 (Microsoft Corp.) was used to perform the data statistics on the physical and chemical properties of the functional soil and the growth status of oatgrass. IBM SPSS Statistics 27.0 was used for analysis of variance and Duncan's test was employed to test the differences in the physical and chemical properties of the functional soils with different ratios ($p < 0.05$). Origin 2021 (Origin Lab) was used to produce the trend charts of the indicators.

3 Results

3.1 Changes in pH and EC of functional soils with different ratios

The pH and EC of functional soils with different ratios and incubation times were measured. With the increase in incubation time, Figure 1A shows that the pH of the functional soil initially followed a sharp downward trend, and the change was not significant after 10 days. At 30 d, the pH of functional soil was 3.70%–16.78% lower than that of CK. Under the same incubation time, with the increase in the GS and CG contents, the pH of the functional soil gradually decreased. After 30 d, the pH ranged from 7.94 to 9.54. In particular, the pH values of FGC3 and FGC4 were 8.54 and 8.25, respectively, which were close to that of SL (8.46). Figure 1B shows that the EC of the functional soil initially decreased and gradually increased with time. There were no significant differences in the EC of functional soil at 10 and 20 d, and values increased significantly at 30 d. At 0 d, the EC was 12.91%–55.12% lower than that of CK. At 30 d of incubation, the functional soil of FGC4 was relatively low compared to the other functional soils, with an EC of 840 μS·cm^{-1}.

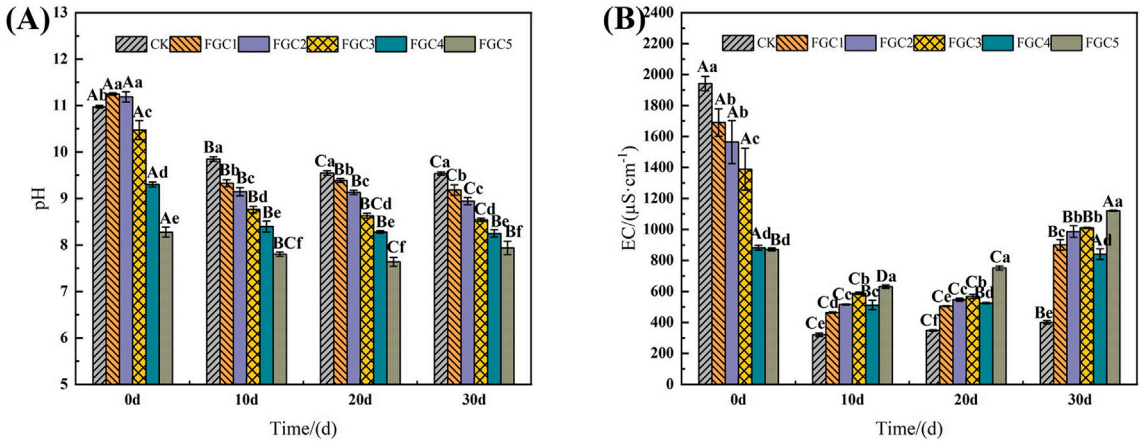

FIGURE 1
Changes in functional soils pH and EC. **(A)** Changes in functional soils pH. **(B)** Changes in functional soils EC. Columns labeled with the same letter are not significantly different at $p < 0.05$. The same lowercase letter means that the difference between the experimental groups with different proportions is not significant during the same action time; The same capital letter indicates that the same proportion of the experimental groups have no significant difference in different action times. Each mean is accompanied by a standard error (n = 3).

Functional soil pH showed a decreasing trend after 10 d compared to 0 d, which can be attributed to the replenishment of the soil with water every 2 days during the experimental period. As a consequence, the base ions in the soil solution moved downward with the water. Moreover, the H^+ in the solution replaced the metal ions on the soil absorption complex and was adsorbed by the soil. This resulted in a decrease in base saturation, an increase in hydrogen saturation, and a decrease in the pH in the functional soil. The gradual decrease in the pH of the functional soil with the increase in CG is attributed to the production of SO_4^{2-} and H^+ during the oxidation and dissolution of iron sulfide. The hydrolysis of sulfate minerals can also reduce the pH of the functional soil (Ma et al., 2020). The specific reaction process is shown in Equations 9–11. Sulfur in CG usually exists in the form of sulfate, pyrite, and organic sulfur, which leads to a decrease in pH (Yang X. et al., 2024). GS also contains different minerals and elements, among which aluminosilicate accounts for more than 60% of the total mineral components (Zhao et al., 2024). These elements may be released in gaseous or dissolved form during the gasification process, thereby reducing the pH value.

$$2FeS_2 + 7O_2 + 2H_2O \rightarrow 2Fe^{2+} + 4SO_4^{2-} + 4H^+ \quad (9)$$

$$Al_2(SO_4)_3 + 6H_2O \rightarrow 2Al(OH)_3 + 3SO_4^{2-} + 3H^+ \quad (10)$$

$$FeSO_4 + H_2O \rightarrow Fe(OH)_3 + SO_4^{2-} + 3H^+ \quad (11)$$

With the decrease of FA and the increase of CG, EC of functional soil gradually decreased before cultivation without watering (0 d). This was due to the decrease in FA content, which reduced the soluble salts SO_4^{2-}, Cl^-, Ca^{2+}, Mg^{2+}, and K^+ in FA (Ukwattage et al., 2021), thereby lowering the salt content of the functional soil. Moreover, with the increase in GS content, soil salinization weakened and EC decreased, which is consistent with the results of Zhang et al. (Zhang R. et al., 2022). However, after 10 d of functional soil action, a small amount of CaO in CG reacted with water in the soil to form $Ca(OH)_2$, causing the functional soil EC to slightly increase with the increase in CG (Shu et al., 2024; Yaofei et al., 2024).

3.2 Changes in nutrient content of functional soils with different ratios

The changes in the nutrient content of functional soil with different ratios are shown in Figure 2. No significant differences are observed in the functional soil organic matter with time. Under the same cultivation time, the functional soil organic matter showed a gradually increasing trend with the increase in CG by 2.49%–10.66%, 2.64%–11.06%, and 2.57%–10.91% at 10, 20, and 30 d, respectively. The functional soil organic matter of FGC3 was higher than that of SL (6.19%) (Figure 2A). At 0, 10, 20, and 30 d, functional soil available phosphorus content gradually decreased with the increase in the GS and CG contents by 26.94–167.74 $mg \cdot kg^{-1}$, 32.80–172.86 $mg \cdot kg^{-1}$, 34.23–155.68 $mg \cdot kg^{-1}$, and 28.37–161.57 $mg \cdot kg^{-1}$, respectively. The effective phosphorus content of the functional soil increased and then decreased with time at the same ratios (Figure 2B). Functional soil available potassium content did not change significantly at 0 d and 30 d, increasing by 13.97%–168.57% and 47.16%–161.89% at 10 d and 20 d, respectively, compared with CK, and decreasing significantly at 30 d by 46.60%–66.05% (Figure 2C). Functional soil ammonium nitrogen content decreased sharply after 10 d and was 66.27%–92.53% lower at 30 d than at 0 d. However, functional soil ammonium nitrogen content was higher than that of CK at 10 d, 20 d, and 30 d (Figure 2D).

CG contains more organic carbon and nutrients, so the organic matter content of functional soil gradually increased with the increase of CG content. And the main reason for the decrease in available phosphorus content of functional soils compared to CK is that the content of available phosphorus in GS and CG is lower than that in FA, as shown by the previous tests. On the other hand, the phosphorus in CG exists in the form of insoluble phosphate, and the content of soluble available phosphorus is extremely low (Zhu et al., 2022). The content of available potassium in functional soil is higher than that in CK, because the mineral composition of CG contains minerals with large amounts of potassium, such as mica and

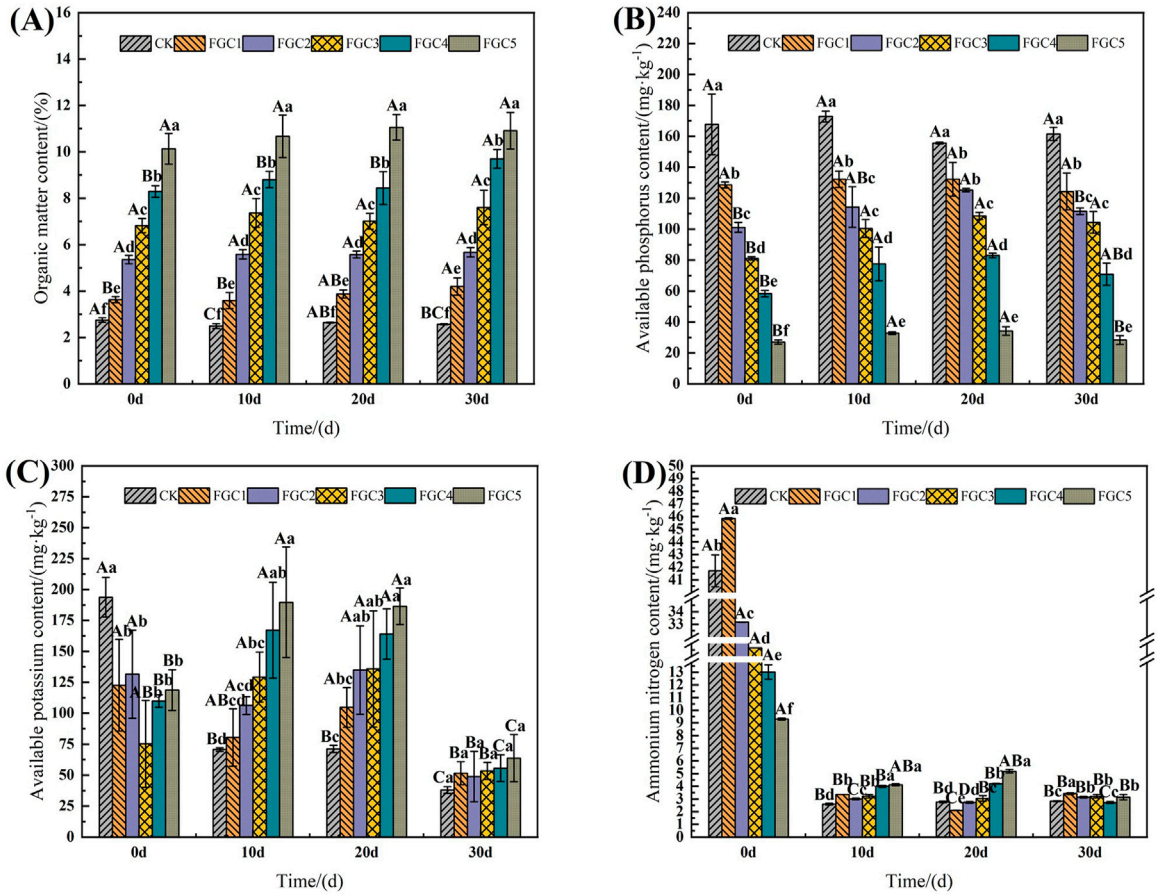

FIGURE 2
Changes in the nutrient content of the functional soils. **(A)** Changes in functional soils organic matter. **(B)** Changes in functional soils available phosphorus. **(C)** Changes in available potassium of the functional soils. **(D)** Changes in functional soils ammonium nitrogen. Columns labeled with the same letter are not significantly different at the $p < 0.05$ level. The same lowercase letter means that the difference between the experimental groups with different proportions is not significant during the same action time; The same capital letter indicates that the same proportion of the experimental groups have no significant difference in different action times. Each mean is accompanied by a standard error (n = 3).

feldspar, which can be decomposed into available potassium (Shu et al., 2024). The sharp decrease in the ammonium nitrogen content of the functional soils at 10, 20, and 30 d compared with that at 0 d may be due to the loss of ammonium nitrogen with the irrigation water.

3.3 Changes in maximum water holding capacity and water loss rate of functional soils with different ratios

Figure 3 shows that the MWH capacity of the functional soil gradually decreased with decreasing FA content and increasing GS and CG contents. The MWH capacity of the functional soil of FGC1, FGC2, and FGC3 was 45.94%, 41.01%, and 36.27%, all of which exceeded those of SL (35.39%). The functional soil water LR gradually increased as FA con-tent decreased. FGC1 exhibited the lowest functional soil moisture LR (except for CK), and the soil LR of FGC1 was 36.89% at 30 d. Moreover, FGC1, FGC2, and FGC3 were significantly lower than SL (53.63%). The experimental results showed that the MWH capacity and water LR of functional soils were related to the contents of FA, GS, and CG.

As the FA content decreased and the GS and CG contents increased, the MWH capacity of functional soil gradually decreased and the water LR gradually increased. This is due to the small particle size of FA, which is rich in specific surface area and pore structure (An et al., 2024). Thus, the decrease in FA can reduce the water-holding capacity of the soil, in addition, the larger particle size and lower capillary porosity of GS can lead to poor soil structure and water retention (Du et al., 2020).

3.4 Changes in bulk density and porosity of functional soils with different ratios

Figure 4 shows that the functional soil bulk density gradually increased with the decrease in FA proportion during the same time period. There were no significant changes in the functional soil bulk density of FGC1 compared with that of CK at 10, 20, and 30 d. For GS and CG contents greater than 5wt%, the soil bulk density increased significantly, and at 30 d, the FGC2, FGC3,

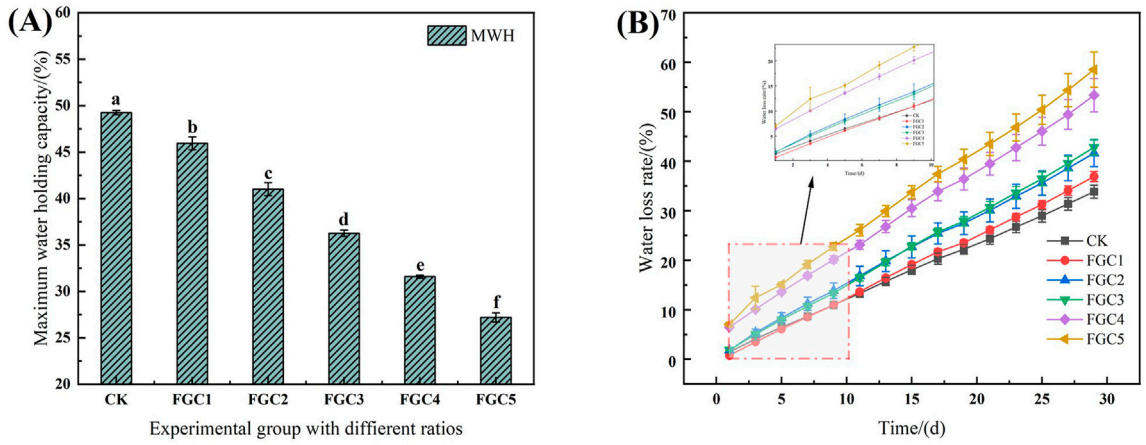

FIGURE 3
Changes in the maximum water-holding capacity and loss rates of functional soils. **(A)** Change in the maximum water-holding capacity of the functional soils. **(B)** Change in the water loss rate of the functional soils. Columns labeled with the same letter are not significantly different at the $p < 0.05$ level. Each mean is accompanied by a standard error (n = 3).

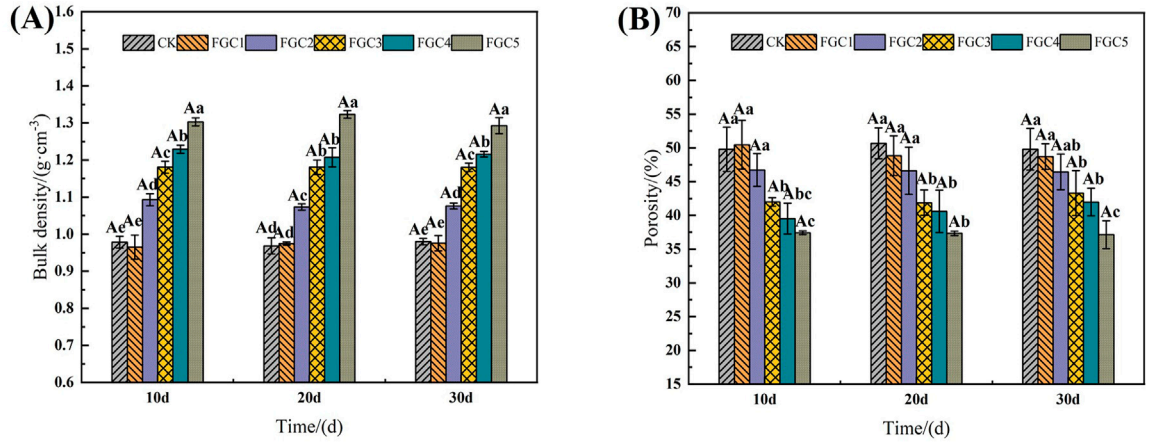

FIGURE 4
Changes in functional soils bulk density and porosity. **(A)** Change in functional soils bulk density. **(B)** Change in functional soils porosity. Columns labeled with the same letter are not significantly different at the $p < 0.05$ level. The same lowercase letter means that the difference between the experimental groups with different proportions is not significant during the same action time; The same capital letter indicates that the same proportion of the experimental groups have no significant difference in different action times. Each mean is accompanied by a standard error (n = 3).

FGC4, and FGC5 functional soil bulk density increased by 9.79%, 20.41%, 24.06%, and 31.91%, respectively, compared with CK at 30 d (Figure 4A). At 10 d, the functional soil bulk density varied from 37.43% to 50.47%, and when the proportion of GS and CG was greater than 5wt%, the functional soil bulk density gradually decreased by 6.15%–24.84% compared to that of CK (Figure 4B). However, there were no significant differences between the functional soil bulk density and porosity of different ratios over time, indicating that the incubation time had little effect on soil bulk density and porosity. At 30 d, the bulk density and porosity of the FGC3 functional soil were close to and greater than those of SL, which had a bulk density of 1.31 g•cm^{-3} and a porosity of 41.99%.

3.5 Changes in solid-liquid-gas ratio of functional soils with different ratios

Figure 5 presents the changes in the ratio of the three functional soil phases (solid, liquid, and gas). As the GS and CG contents increased, the solid phase of the functional soil gradually increased and the gas phase gradually decreased. At 10 d, the solid phase of FGC1 was 1.35% lower than that of CK, the liquid phase was 26.22% higher, and the gas phase was 17.45% lower. Also at 10 d, the solid phase of FGC1, FGC2, and FGC3 decreased by 14.62%, 8.18%, and 0.03%, respectively, compared with SL. Thus, the FGC3 value was closer to the proportion of the SL solid phase (58.1%), while the gas phase was higher than that of SL (12.59%). The functional soil

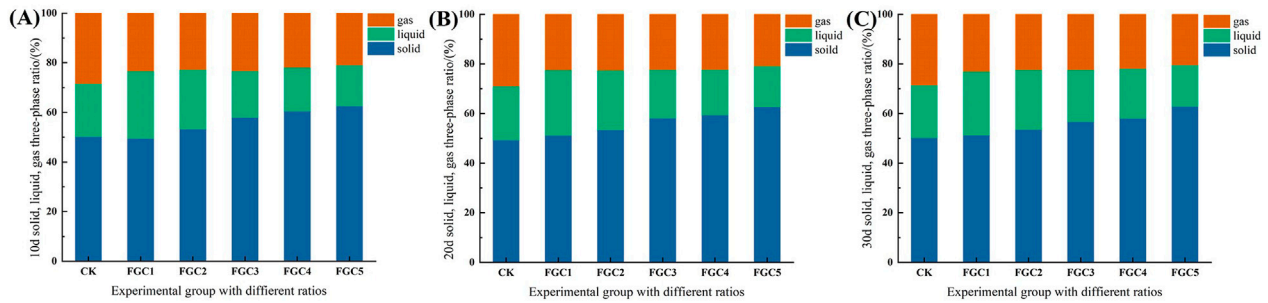

FIGURE 5
Variation of the solid, liquid, and gas phase percentages of the functional soils. **(A)** 10 d changes in the solid, liquid, gas three-phase ratio. **(B)** 20 d changes in the solid, liquid, gas three-phase ratio. **(C)** 30 d changes in the solid, liquid, gas three-phase ratio.

solid-liquid-gas phase ratios did not change significantly with time. The soil three-phase ratio is an important indicator of soil physical properties, reflecting the compactness, water content, and aeration of the soil (Yang S. et al., 2024). The solid, liquid, and gas phases of the functional soil changed with the bulk density and porosity. In general, the smaller the bulk density of the functional soil, the larger the porosity, corresponding to a decrease in the solid phase of the soil and an increase in the liquid and gas phases.

3.6 Analysis of plant agronomic traits

Figures 6A–D shows that the plant height, stem thickness, fresh weight, and dry weight of oatgrass initially increased and subsequently decreased with the increase in the GS and CG contents. The overall plant height of oatgrass at 30 d ranged from 17.68 to 30.3 cm, with the heights of FGC3, FGC4, and FGC5 increasing by 52.97%, 71.30%, and 57.65%, respectively, compared with CK. FGC3 plants (FA at 50wt%, and GS and CG at 25wt%) exhibited the best growth characteristics, namely, the stem thickness, fresh weight, and dry weight increased by 26.81%, 172.78%, and 148.15%, respectively, compared with CK. As the GS and CG contents increased, the plant chlorophyll content, which varied between 22.9 and 28.3 SPAD, was 7.78%–23.35% higher than CK. The highest chlorophyll content was observed for FGC1 and FGC3 oatgrass (Figure 6E). Figure 7 compares the growth of oatgrass planted in different ratios of functional soils.

The main components of FA, GS, and CG are Al_2O_3 and SiO_2, which are similar to clay. FA also contains trace elements required by plants, such as B, Fe, Mo, Cu, Mn, and Zn. In addition, an appropriate amount of CG can improve the nutrient content of functional soil and provide a good growth environment for plants. The trace elements contained in CG can also promote crop growth and development. However, the particle size of CG is large and the porosity is low. Excessive CG will destroy the functional soil matrix and water retention (Du et al., 2020), which is not conducive to plant growth. Our results show that an appropriate amount of GS and CG can reduce the pH of functional soil and increase the nutrient content. The improvement of the chemical properties of functional soil provides a suitable environment for plant growth and the absorption of nutrients by the roots.

4 Discussion

The development and utilisation of mineral resources have resulted in a large area of mine abandonment and serious destruction of surface vegetation, and the amount of coal-based solid waste generated far exceeds the amount of comprehensive utilisation. In this case, the preparation of coal-based solid waste functional soil is very important for ecological restoration in mining area and promoting the green development of mining industry. FA has a small particle size, a large specific surface area, low bulk density, and high water-holding capacity, which helps to improve the water-holding capacity and texture of the soil and facilitates nutrient absorption by plants (Usman et al., 2023). GS can increase the pores between functional soil particles, loosen the soil texture, improve soil permeability, accelerate the downward movement of water, and reduce soil salinization (Yin et al., 2022). Sulphate and silicate in CG can reduce soil pH, and CG contains a high content of organic matter (Liu et al., 2024). In addition, the main components of FA, GS, and CG are Al_2O_3 and SiO_2, which are similar to natural clay and contain trace elements required by plants. Therefore, it is feasible to prepare functional soil with the three coal-based solid wastes of FA, GS, and CG.

With the increase of GS and CG, the pH of functional soil gradually decreased after 30 days of cultivation, mainly because the pyrite (FeS_2) in CG would be oxidized to sulfate ion, thus reducing the pH value of functional soil (Cheng et al., 2014), which was consistent with the findings of Shu et al. (2024). The pH range of oat grass suitable for growth is 6.0–8.5, and higher or lower pH value will increase biological toxicity and inhibit plant growth. Moreover, after 10 d of functional soil action, a small amount of CaO in CG reacted with water in the soil to form $Ca(OH)_2$, causing the functional soil EC to slightly increase with the increase in CG (Shu et al., 2024; Yaofei et al., 2024). The gradual increase in soil organic matter content with the increase in CG can be attributed to the large amount of carbonaceous shale or carbonaceous siltstone in the gangue, which contains 15%–20% organic matter. The addition of CG will increase the organic matter content of the soil and provide the necessary nutrient content for plant growth. Our findings are in consistent with those of Du et al. (2020). Available phosphorus and available potassium in the soil can be directly absorbed and utilized by plants. With the increase in CG, the available phosphorus content of functional soil decreased significantly. This is because the

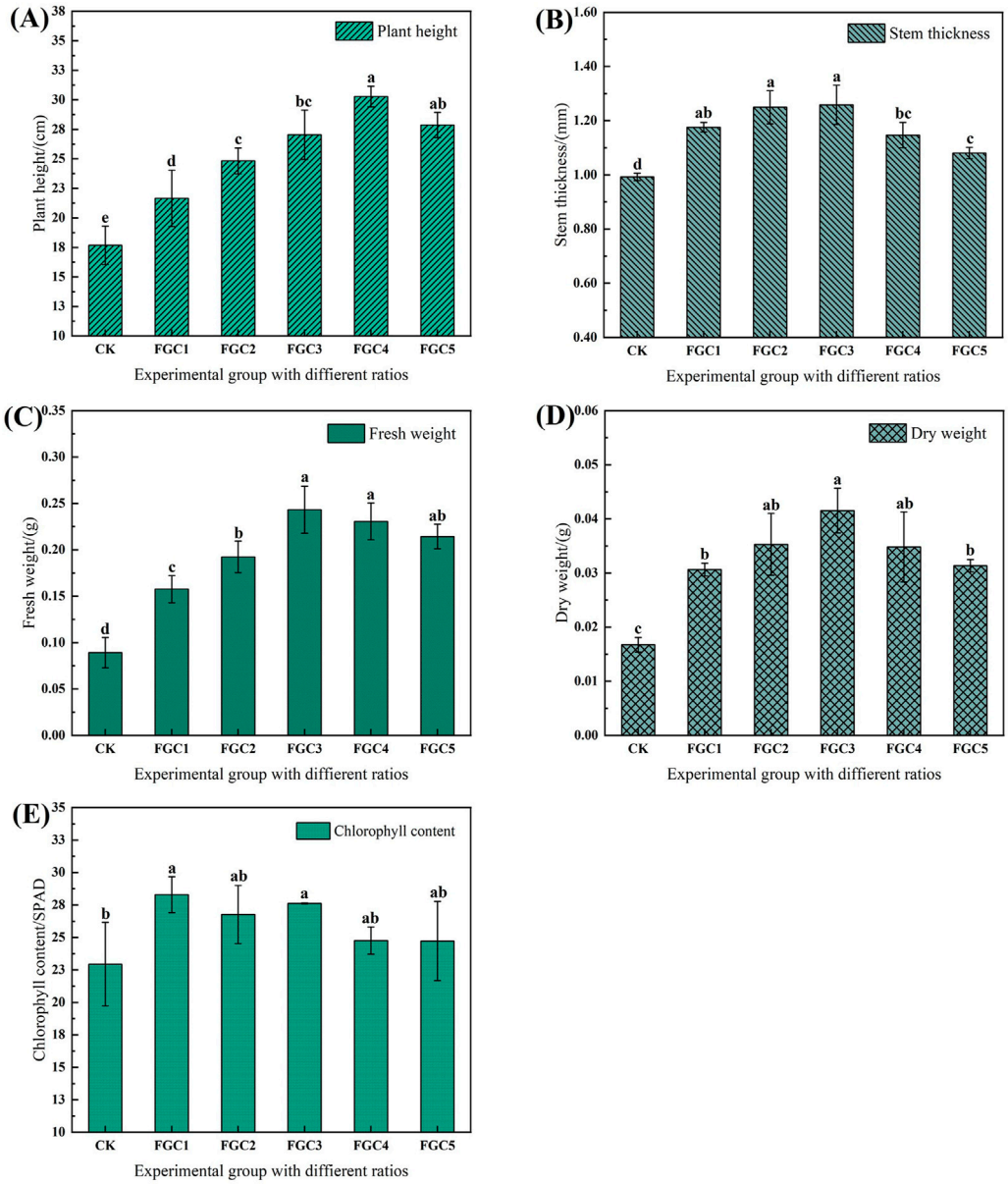

FIGURE 6
Effect of different functional soil ratios on plant growth. **(A)** Change in plant height. **(B)** Change in stem thickness. **(C)** Change in fresh weight. **(D)** Change in dry weight. **(E)** Change in chlorophyll content. Columns labeled with the same letter are not significantly different at the $p < 0.05$ level. Each mean is accompanied by a standard error (n = 3).

phosphorus in CG mainly exists in the form of insoluble phosphate, and the soluble available phosphorus content is extremely low (Zhu et al., 2022). Potassium in gangue mainly exists in dolomite and feldspar, and these minerals can be decomposed into available potassium to be absorbed and utilized by plants, which was consistent with the findings of Zhu et al. (2022) (Shu et al., 2024). Thus, the available potassium content of the cultivated functional soils increased gradually with CG.

As the GS and CG contents increased, the functional soil bulk density increased and porosity decreased. This is because the dense structure of CG reduced the water permeability of the functional soil, while the laminated structure of kaolin minerals in the coal gangue after grinding (pass through a 2 mm aperture sieve) was destroyed. This resulted in the production of a large amount of SiO_2 and Al_2O_3 and a strengthening of the gangue gelling capacity (Chen et al., 2021). Thus, the increase in CG reduced the ratio of impermeable minerals, which increased the bulk density and decreased porosity of the functional soil. Moreover, the decrease in FA content increased the bulk density and reduced the porosity of the functional soil. FA has a small particle size and large specific surface area, which increases the pore structure of functional soil, and the larger specific surface area promotes the contact between particles and water molecules, which improves water retention (Shaheen et al., 2014). In addition, GS coarse aerated slag has a small specific surface area and pore volume, and a large number of aggregated inorganic minerals are present on the pore surface and in

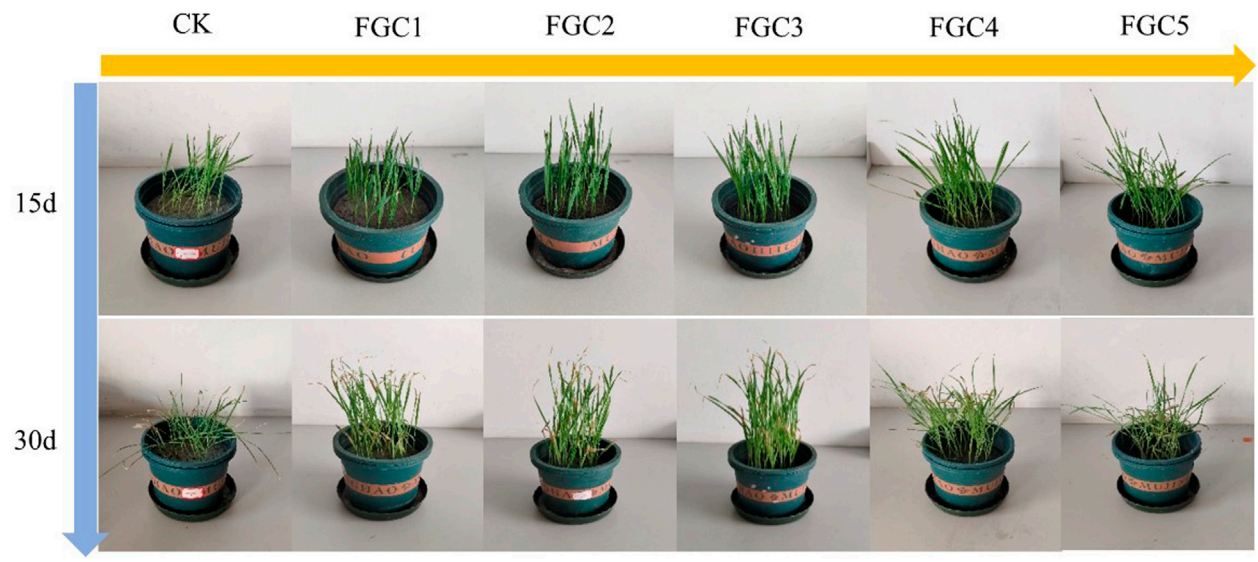

FIGURE 7
Comparison of growth of oatgrass at different times and different functional soil ratios.

the internal pores, thus affecting the water-holding capacity of the functional soil (Liu et al., 2021). Therefore, the decrease in FA content and increase in GS and CG contents reduced the water-holding capacity and enhanced the densification of the soil. The contents of GS and CG should be controlled within an appropriate range. When the GS and CG contents are less than 25wt%, the chemical properties of the functional soil are improved, and physical indicators such as bulk density and porosity are generally close to and better than those of SL.

The results of the oatgrass pot experiment showed that the plant height, stem diameter, fresh weight, and dry weight of oatgrass planted in FGC functional soil under different ratios were higher than those in CK. As the GS and CG contents increased, the plant height, stem diameter, fresh weight, and dry weight of oatgrass initially increased and then decreased. When the content of GS and CG was higher than 25wt%, the chlorophyll content of the plant decreased slightly, but was still higher than that of CK. The decrease in the pH of the functional soil is conducive to the growth of plant roots and the absorption and utilization of nutrients. In addition, the nutrient content of the soil is a key factor in plant growth. The increase in nutrient content in the functional soil is beneficial to the growth and development of plants.

From an economic point of view, functional soil is easier to obtain and cheaper than normal soil. Functional soil raw materials come from coal-based solid waste, which not only solves the problem of coal-based solid waste accumulation, but also promotes the ecological restoration of mining areas, and is conducive to the green and sustainable development of mining areas. However, the limitations of using this method are the need for professional testing of coal-based solid waste materials before restoration, and regular testing of functional soils in the area after restoration to ensure that they do not pollute the soil and groundwater. Therefore, the promotion of this technology has higher requirements.

5 Conclusion

This study develops a new way of utilizing coal-based solid waste, applying the solid waste generated in the process of coal-fired power generation to the ecological restoration of mining areas. In this study, functional soil was prepared using FA, GS, and CG, and the physical and chemical properties of the functional soil and the agronomic traits of oatgrass plants were studied. The preparation of pure solid waste functional soil alleviates the shortage of soil in mining area, and provides guidance for the large-scale utilization of fly ash, gasification slag, coal gangue and ecological restoration in mining area. The main research conclusions are as follows.

(1) With the decrease in FA content and increase in GS and CG contents, the pH of the functional soil was effectively reduced, and the organic matter, available potassium, and ammonium nitrogen nutrient content of the functional soil improved. In addition, when the GS and CG contents were lower than 25wt%, the bulk density and porosity of the functional soils of FGC1, FGC2, and FGC3 were better than those of SL.
(2) Oatgrass plant height, stem thickness, fresh weight, dry weight, and chlorophyll content were all improved, and FGC3 exhibited the best growth. Analysis of the above indicators identified FGC3 as the optimal functional soil ratio, with FA, GS, and CG contents of 50wt%, 25wt%, and 25wt%, respectively.

Data availability statement

The raw data supporting the conclusions of this article will be made available by the authors, without undue reservation.

Author contributions

YL: Formal Analysis, Investigation, Visualization, Writing–original draft, Writing–review and editing. FH: Funding acquisition, Project administration, Supervision, Writing–review and editing. NL: Formal Analysis, Investigation, Writing–review and editing. FD: Formal Analysis, Investigation, Writing–review and editing. CA: Formal Analysis, Writing–review and editing. WY: Supervision, Writing–review and editing. TL: Supervision, Writing–review and editing.

Funding

The author(s) declare that financial support was received for the research, authorship, and/or publication of this article. Major Scientific and Technological Achievements Transformation Project of Ningxia Hui Autonomous Region (2023KJCGZH0242). And the great support of Helanshan Laboratory.

Conflict of interest

The authors declare that the research was conducted in the absence of any commercial or financial relationships that could be construed as a potential conflict of interest.

Generative AI statement

The author(s) declare that no Generative AI was used in the creation of this manuscript.

Publisher's note

References

An, C., Han, F., Li, N., Zheng, J., Li, M., Liu, Y., et al. (2024). Improving physical and chemical properties of saline soils with fly ash saline and alkaline amendment materials. *Sustainability* 16 (8), 3216. doi:10.3390/su16083216

Chao, X., Zhang, T., Lv, G., Zhao, Q., Cheng, F., and Guo, Y. (2023). Sustainable application of coal fly ash: one-step hydrothermal cleaner production of silicon-potassium mineral fertilizer synergistic alumina extraction. *J. Clean. Prod.* 426, 139110. doi:10.1016/j.jclepro.2023.139110

Chen, J., Guan, X., Zhu, M., and Gao, J. (2021). Mechanism on activation of coal gangue admixture. *Adv. Civ. Eng.* 2021. doi:10.1155/2021/5436482

Chen, R., Han, L., Liu, Z., Zhao, Y., Li, R., Xia, L., et al. (2022). Assessment of soil-heavy metal pollution and the health risks in a mining area from southern Shaanxi Province, China. *Toxics* 10 (7), 385. doi:10.3390/toxics10070385

Cheng, W., Bian, Z., Dong, J., and Lei, S. (2014). Soil properties in reclaimed farmland by filling subsidence basin due to underground coal mining with mineral wastes in China. *Trans. Nonferrous Metals Soc. China* 24 (8), 2627–2635. doi:10.1016/s1003-6326(14)63392-6

Du, T., Wang, D., Bai, Y., and Zhang, Z. (2020). Optimizing the formulation of coal gangue planting substrate using wastes: The sustainability of coal mine ecological restoration. *Ecol. Eng.* 143, 105669. doi:10.1016/j.ecoleng.2019.105669

Liu, H., Wang, J., Abiyasi, Li, H., Yin, C., Liu, J., et al. (2022). Effect of coal gasification slag on improving physical properties of acid soil. *Sci. Adv. Mater.* 14 (4), 703–709. doi:10.1166/sam.2022.4261

Liu, X., Jin, Z., Jing, Y., Fan, P., Qi, Z., Bao, W., et al. (2021). Review of the characteristics and graded utilisation of coal gasification slag. *Chin. J. Chem. Eng.* 35, 92–106. doi:10.1016/j.cjche.2021.05.007

Liu, X., Zhang, J., Li, Q., and Liang, W. (2024). Preparation of technosol based on coal gangue and its impact on plant growth in coal mining area. *J. Clean. Prod.* 467, 142998. doi:10.1016/j.jclepro.2024.142998

Luo, C., Li, S., Ren, P., Yan, F., Wang, L., Guo, B., et al. (2024). Enhancing the carbon content of coal gangue for composting through sludge amendment: a feasibility study. *Environ. Pollut.* 348, 123439. doi:10.1016/j.envpol.2024.123439

Ma, J., Quan, Z., Sun, Y., Du, J., and Liu, B. (2020). Excess sulfur and Fe elements drive changes in soil and vegetation at abandoned coal gangues, Guizhou China. *Sci. Rep.* 10 (1), 10456. doi:10.1038/s41598-020-67311-z

Ou, Y., Ma, S., Zhou, X., Wang, X., Shi, J., and Zhang, Y. (2020). The effect of a fly ash-based soil conditioner on corn and wheat yield and risk analysis of heavy metal contamination. *Sustainability* 12 (18), 7281. doi:10.3390/su12187281

Panda, D., Barik, J. R., Barik, J., Behera, P. K., and Dash, D. (2021). Suitability of Brahmi (Bacopa monnieriL.) cultivation on fly ash-amended soil for better growth and oil content. *Int. J. Phytoremediation* 23 (1), 72–79. doi:10.1080/15226514.2020.1791052

Rusanescu, C. O., and Rusanescu, M. (2023). Application of fly ash obtained from the incineration of municipal solid waste in agriculture. *Appl. Sciences-Basel* 13 (5), 3246. doi:10.3390/app13053246

Shaheen, S. M., Hooda, P. S., and Tsadilas, C. D. (2014). Opportunities and challenges in the use of coal fly ash for soil improvements - a review. *J. Environ. Manag.* 145, 249–267. doi:10.1016/j.jenvman.2014.07.005

Shu, L., Wang, H., and He, X. (2024). Physicochemical properties and planting performance of artificial soil developed from multiple coal-based solid waste materials. *Sustainability* 16 (5), 1955. doi:10.3390/su16051955

Shuai, H., Tian, S., Jin, B., Wang, Z., Wang, J., Zhang, Y., et al. (2022). Effects of Vetiveria zizanioides on the restoration and succession of coal gangue mountain plant communities in different years. *Diversity-Basel* 14 (10), 843. doi:10.3390/d14100843

Ukwattage, N. L., Lakmalie, U. V., and Gamage, R. P. (2021). Soil and plant growth response and trace elements accumulation in sweet corn and snow pea grown under fresh and carbonated coal fly ash amendment. *Agron. J.* 113 (4), 3147–3158. doi:10.1002/agj2.20711

Usman, M., Anastopoulos, I., Hamid, Y., and Wakeel, A. (2023). Recent trends in the use of fly ash for the adsorption of pollutants in contaminated wastewater and soils: effects on soil quality and plant growth. *Environ. Sci. Pollut. Res.* 30 (60), 124427–124446. doi:10.1007/s11356-022-19192-0

Vinayagam, S., Sathishkumar, K., Ayyamperumal, R., Natarajan, P. M., Ahmad, I., Saeed, M., et al. (2024). Distribution and transport of contaminants in soil through mining processes and its environmental impact and health hazard assessment: a review of the prospective solutions. *Environ. Res.* 240, 117473. doi:10.1016/j.envres.2023.117473

Wang, C., and Cheng, L. (2024). Study on general industrial solid waste and carbon reduction in China: coupling coordination model, life cycle assessment and environmental safety control. *Sustain. Chem. Pharm.* 39, 101557. doi:10.1016/j.scp.2024.101557

Xu, H., Xu, F., Lin, T., Xu, Q., Yu, P., Wang, C., et al. (2023). A systematic review and comprehensive analysis on ecological restoration of mining areas in the arid region of China: challenge, capability and reconsideration. *Ecol. Indic.* 154, 110630. doi:10.1016/j.ecolind.2023.110630

Yang, S., Wang, Z., Yang, C., Wang, C., Wang, Z., Yan, X., et al. (2024a). Estimation of generalized soil structure index based on differential spectra of different orders by multivariate assessment. *Int. Soil Water Conservation Res.* 12 (2), 313–321. doi:10.1016/j.iswcr.2023.08.008

Yang, X., Yue, C., Wang, Y., Wang, J., Chang, L., and Bao, W. (2024b). A study on the occurrence modes and distribution characteristics of sulfur and mercury in coal gasification slag. *Fuel* 374, 132423. doi:10.1016/j.fuel.2024.132423

Yaofei, L., Xingchen, Z., and Ke, Z. (2024). Coal gangue in asphalt pavement: a review of applications and performance influence. *Case Stud. Constr. Mater.* 20, e03282. doi:10.1016/j.cscm.2024.e03282

Yin, C., Zhao, J., Liu, X., Yu, Z., and Liu, H. (2022). Effect of coal water slurry gasification slag on soil water physical characteristics and properties in saline-alkali soil improvement. *J. Sensors* 2022, 1–11. doi:10.1155/2022/1114343

Yuan, M., Ouyang, J., Zheng, S., Tian, Y., Sun, R., Bao, R., et al. (2022). Research on ecological effect assessment method of ecological restoration of open-pit coal mines in alpine regions. *Int. J. Environ. Res. Public Health* 19 (13), 7682. doi:10.3390/ijerph19137682

Zhang, J., Yang, K., He, X., Wei, Z., Zhao, X., and Fang, J. (2022a). Experimental study on strength development and engineering performance of coal-based solid waste paste filling material. *Metals* 12 (7), 1155. doi:10.3390/met12071155

Zhang, J., Yang, K., He, X., Zhao, X., Wei, Z., and He, S. (2024). Research status of comprehensive utilization of coal-based solid waste (CSW) and key technologies of filling mining in China: a review. *Sci. Total Environ.* 926, 171855. doi:10.1016/j.scitotenv.2024.171855

Zhang, K., Song, S., Zhao, J., Li, X., and Liu, C. (2023). Land reclamation using typical coal gasification slag in Xinjiang: a full-cycle environmental risk study. *Minerals* 13 (10), 1263. doi:10.3390/min13101263

Zhang, R., Li, X., Zhang, K., Wang, P., Xue, P., and Zhang, H. (2022b). Research on the application of coal gasification slag in soil improvement. *Processes* 10 (12), 2690. doi:10.3390/pr10122690

Zhao, J., Yu, T., Zhang, H., Zhang, Y., Ma, L., Li, J., et al. (2024). Study on extraction valuable metal elements by co-roasting coal gangue with coal gasification coarse slag. *Molecules* 29 (1), 130. doi:10.3390/molecules29010130

Zhu, D., Zuo, J., Jiang, Y., Zhang, J., Zhang, J., and Wei, C. (2020). Carbon-silica mesoporous composite *in situ* prepared from coal gasification fine slag by acid leaching method and its application in nitrate removing. *Sci. Total Environ.* 707, 136102. doi:10.1016/j.scitotenv.2019.136102

Zhu, X., Gong, W., Li, W., Bai, X., and Zhang, C. (2022). Reclamation of waste coal gangue activated by Stenotrophomonas maltophilia for mine soil improvement: solubilizing behavior of bacteria on nutrient elements. *J. Environ. Manag.* 320, 115865. doi:10.1016/j.jenvman.2022.115865